Hindawi
Advances in Materials Science and Engineering
Volume 2017, Article ID 2479507, 10 pages
https://doi.org/10.1155/2017/2479507

Research Article

Dynamic Behavior of Clay-Aggregate Mixtures

Kang Fei and Jinxin Xu

Institute of Geotechnical Engineering, Yangzhou University, Yangzhou 225127, China

Correspondence should be addressed to Kang Fei; kfei@yzu.edu.cn

Received 6 December 2016; Accepted 26 January 2017; Published 16 February 2017

Academic Editor: Philip Eisenlohr

Clay-aggregate mixtures are frequently used in engineering practice. To improve the understanding of the effects of coarse particles on the dynamic behavior of clay-aggregate mixtures, series of stress controlled cyclic triaxial tests were performed on clay specimens with various glass bead contents. The results show that the initial shear modulus of clay-aggregate mixtures increased with the increase of the coarse aggregate content and the confining stress. At the confining stress of 100, 200, and 400 kPa, the addition of 32% coarse particles caused an increase in the initial shear modulus of 117%, 110%, and 67%, respectively. Moreover, the normalized shear modulus decreased and damping ratio increased with the coarse aggregate content, and the influence of the confining stress on the strain-dependent dynamic properties was negligible. The specimen with a higher coarse aggregate content was observed to have larger cyclic shear strength and smaller excess pore water pressure, but the effects of the coarse aggregate content became less pronounced under large cyclic stresses.

1. Introduction

Clay-aggregate mixtures refer to clays mixed with sand, gravel, or cobble particles. These types of composite soils are frequently used in engineering practice. For example, to improve the strength and stiffness of the core of earth dams, a certain amount of gravels is usually added to the clay. A complete understanding of the dynamic behavior of such composite materials is very important for engineering applications.

In the past, studies of the dynamic behavior of soil mixtures have concentrated mostly on the effects of clay content on the cyclic shear strength of clay-sand mixtures. Thevanayagam et al. [1] reported that the increasing fines content resulted in a decrease in the resistance to liquefaction. Chien et al. [2] stated that the liquefaction resistance decreased with the fines content under the constant relative density. However, Kuwano et al. [3] concluded that the liquefaction resistance increased with the clay content based on the results of cyclic triaxial tests. Ovando-Shelley and Pérez [4] also suggested that the addition of clay increased the liquefaction potential of kaolin-sand mixtures. The influences of the clay plasticity on the strength increment were studied by Ishihara [5], Beroya et al. [6], and Park and Kim [7]. Many other researchers observed that the cyclic shear strength decreased with the fines content at first. Beyond a transition fines content, the strength increased with a further increase in fines content [8–11].

The conflicting pattern observed in the cyclic shear strength with the clay content is a reflection of the roles of clay and coarse particles in the load transfer [12, 13]. Cabalar and Mustafa [14, 15] pointed out that the mechanical behavior of sand-clay mixtures depended on the relative concentration of the sand and clay samples. When the clay content is low, the coarse particles are in contact with others, and the formed coarse particle structure dominates the dynamic behavior, whereas the clay fraction acts only to fill the voids between coarse particles. For this case, the intergranular void ratio was suggested to use to describe the behavior of the soil mixture [16–19]. In contrast, when the clay content is high, coarse particles are floated in the clay matrix and the overall behavior is controlled by the clay fraction. The mechanical behavior of the soil mixture is expected to be similar to that of the pure clay with the same interfine void ratio [20]. However, Yagiz [21], Zhao et al. [22], and Fei [23] pointed out that the coarse particles still have a significant influence on the strength of clay-aggregate mixtures, even if the coarse aggregate content is not high enough to form a stable skeleton.

The strain-dependent dynamic deformation characteristics of clay-aggregate mixtures have also attracted the attention of researchers. On the basis of the results of dynamic hollow cylinder tests, Yamada et al. [24, 25] have suggested empirical relationships to estimate the strain-dependent shear modulus and damping ratio of clay-sand mixtures. In the proposed method, the effects of sand content were accounted by the equivalent plasticity index. But, for clay-gravel mixtures, the plasticity index cannot be obtained by conventional laboratory tests due to the existence of coarse particles. Shafiee and Ghate [26] observed that both the initial shear modulus and the damping ratio increase with the increase in coarse aggregate content, while the opposite trend was observed for the normalized shear modulus at different strain levels. However, a different pattern in dynamic properties with the coarse aggregate content was observed by Meidani et al. [27]. They concluded that the samples with higher gravel content have higher normalized shear modulus and lower damping ratio. One possible reason is that the gravels were in contact with others under the tested gravel content, and the formed gravel structure dominated the dynamic behavior.

As reviewed, the dynamic behavior of clay-aggregate mixtures has not been comprehensively studied yet, especially for the soil mixtures with moderate coarse aggregate contents. For example, the published experimental data of composite clay cores are very limited. To obtain a full understanding of the effects of the coarse particles on the dynamic characteristics of clay-aggregate mixtures, stress controlled cyclic triaxial tests were carried out in this study. On the basis of the test results, the effects of the coarse aggregate content on the strain-dependent shear modulus, the damping ratio, the dynamic pore water pressure, and the cyclic strength were analyzed.

2. Experimental Program

2.1. Test Materials. The clay used in the investigation was kaolinite. Its liquid limit and plastic limit were 43 and 21, respectively. The specific gravity of the clay was 2.62. For all the specimens, the dry density of the clay was kept constant at 1.55 g/cm^3; in other words, the interfine void ratio was constant. The sampling water content of the clay was 21%.

Glass beads were used as the coarse particles added to the clay. The specific gravity of the glass beads was 2.54, which is similar to that of natural gravels. The diameter of the glass beads is 1.4 cm. The main purpose of using the uniform-sized glass beads was to eliminate the effects of shape and graduation of coarse particles. The volume of the glass beads relative to the total volume of the mixture P was selected as 0, 8%, 16%, 24%, and 32%, respectively. These coarse aggregate contents cover the normal range used in the composite clay core of dams.

2.2. Specimen Preparation and Test Procedure. The cyclic triaxial tests were performed by GDS dynamic triaxial system. The specimens were 10 cm in diameter and 20 cm in height. All the test specimens were prepared by a moist tamping technique. First, the glass beads were mixed with the dry clay based on the designated coarse aggregate content. Then, the required amount of water was added to the soil mixture, and the soil was mixed thoroughly to ensure homogeneous distribution of coarse particles. Subsequently, the mixed soil was kept inside a plastic bag for 3 days to moisture homogenization. Afterwards, the soil was compacted using a 2.5 kg rammer to the desired dry density of the clay. The number of rammer blows was determined by trial and error. After the compaction, the specimens were saturated by vacuum-pumping for 24 h.

Two series of cyclic triaxial tests were performed in this study. The first series was used to determine the strain-dependent modulus and the damping ratio of clay-aggregate mixtures. In these tests, the specimens were first isotropically consolidated to an initial effective confining stress σ_0' of 100, 200, and 400 kPa. Then, the specimens were subjected to sinusoidal undrained cyclic loading at a frequency of 0.1 Hz and 10 cycles were applied in each loading stage. The small loading frequency was chosen to ensure the equalization of the pore water pressure in the sample. At the end of each loading step, the drainage valve was opened to dissipate the excess pore water pressure. The second series was used to determine the cyclic strength of clay-aggregate mixtures. For this purpose, undrained cyclic stresses with different amplitudes were applied after consolidation. In this series of tests, σ_0' was fixed at 100 kPa, and only the specimens with 0, 16%, and 32% coarse particles were tested. The loading frequency was 0.1 Hz, and the cyclic stress ratio CSR (half of the cyclic deviator stress divided by the effective confining stress $\sigma_d/2\sigma_0'$) ranged from 0.1 to 0.3. The failure condition of the sample was defined as a double amplitude strain of 5%.

3. Test Results

3.1. Initial Shear Modulus. By connecting the extreme points of the cyclic shear stress-shear strain hysteresis loops under different loading stages, the skeleton curves at various coarse aggregate contents can be obtained. The results of the specimens with 0% and 32% coarse aggregates are shown in Figure 1, where τ is the shear stress and γ is the shear strain. As observed, the nonlinear characteristics of the backbone curves are obvious and the hyperbolic model can be used to describe the stress-strain response. Similar results were also found for other coarse aggregate contents. By using the hyperbolic model, the initial shear modulus G_0 (the tangential slope of the backbone curve when the strain is zero) can be determined. The obtained relationships between the initial shear modulus and the coarse aggregate content at various initial confining stresses are shown in Figure 2.

It is generally believed that the mechanical behavior of clay-aggregate mixtures is mainly governed by the clay matrix up to a transition coarse aggregate content [28]. This transition coarse aggregate content is usually estimated by the maximum possible void ratio of the coarse grains. Based on the research of McGeary [29], the transition content is 53.36% for the case of one-size spheres packed in a simple cubic pattern. This value is significantly larger than those adopted in this study. It implies that the initial shear modulus of the tested clay-aggregate mixtures should be close to that

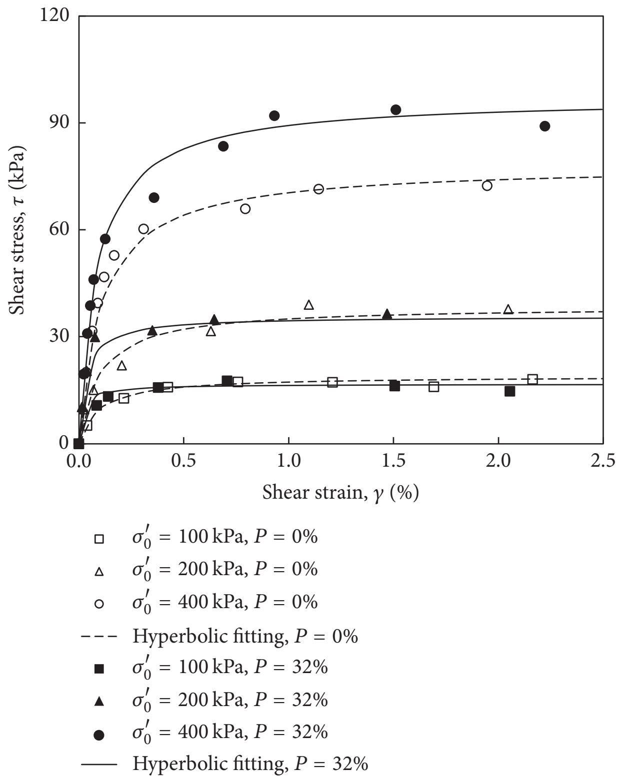

Figure 1: Backbone curve of clay-aggregate mixture.

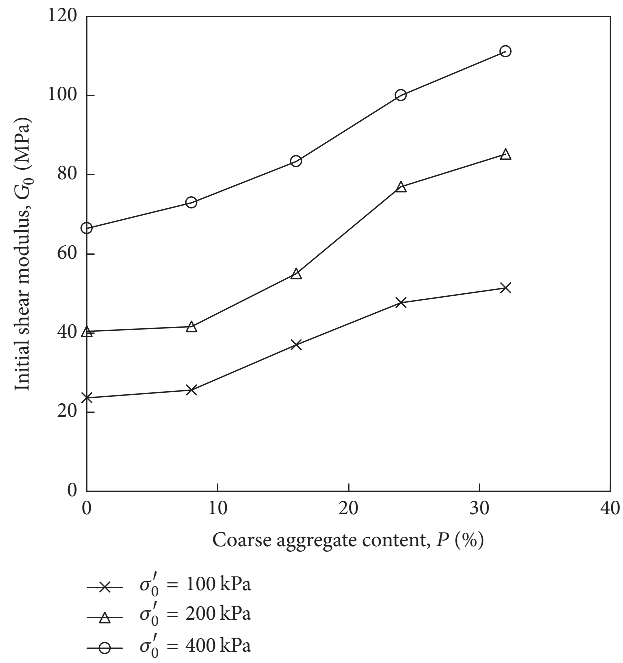

Figure 2: Relationship between initial shear modulus and coarse aggregate content.

Table 1: List of values of A, B, and n for various data sources.

	A	B	n
This study	400	1.60	0.60
Yamada et al. [24]	49	5.13	0.50
Meidani et al. [27]	380	2.00	0.59

of pure clay, and the effect of the coarse aggregate content is negligible. However, Figure 2 shows that the coarse aggregate content still has a remarkable effect on the initial shear modulus, even though the dry density of the clay fraction was kept constant. At the confining stress of 100, 200, and 400 kPa, the addition of 32% coarse particles caused an increase in the initial shear modulus of 117%, 110%, and 67%, respectively. This phenomenon can be explained from the point of the view of force chains. For the specimens with relatively low coarse aggregate contents, the coarse particles were far away from each other; the dynamic behavior was controlled by the clay. When more coarse particles were added to the host clay, the coarse particles made active contacts with the clay grains and the force chain consisted of clay and coarse particles together. In addition, the coarse particles also introduced kinematic constrains for deformation of the surrounded clay. Therefore, the larger coarse aggregate content led to a stronger force chain and a higher initial shear modulus.

Within the adopted coarse aggregate contents in this study, both coarse particles and clay grains participate actively in the force chain, so the global void ratio is expected to be an index of active contacts. The variations of the initial shear modulus versus the global void ratio at different confining stress are shown in Figure 3. As can be seen, there is a good agreement and a definite trend between the initial shear modulus and the global void ratio. It is therefore possible to estimate the initial shear modulus in terms of the global void ratio and the effective confining stress in the same way as that for clays [30]. Thus, the initial shear modulus of clay-aggregate mixtures can be expressed in the following form:

$$G_0 = A\frac{(B-e)^2}{1+e}p_a\left(\frac{\sigma_0'}{p_a}\right)^n, \tag{1}$$

where p_a is atmospheric pressure; e is global void ratio. A, B, and n are material constants to be determined experimentally. Based on the test results, the values of A, B, and n were taken as 400, 1.60, and 0.60, respectively. The predicted initial shear moduli using (1) were represented by lines in Figure 3. It is observed that there is a good correlation between the predicted and the measured values. It should be noted that because the dry density of the clay matrix of all specimens remained constant, the addition of coarse particles reduced the global void ratio. Hence, the effect of coarse aggregate content is represented by the global void ratio in (1).

To further verify the reliability of the proposed approach, the test data from literature are compared with the predicted results in Figure 4. The material constants used in the prediction are shown in Table 1. In the study of Yamada et al. [24], a series of cyclic hollow cylindrical torsional shear tests were carried out on clay-sand mixtures. The mean size of the sand particles was 1 mm. In the cyclic triaxial tests conducted by Meidani et al. [27], the coarse particles added to the clay were gravels with an average size of 7.1 mm. In

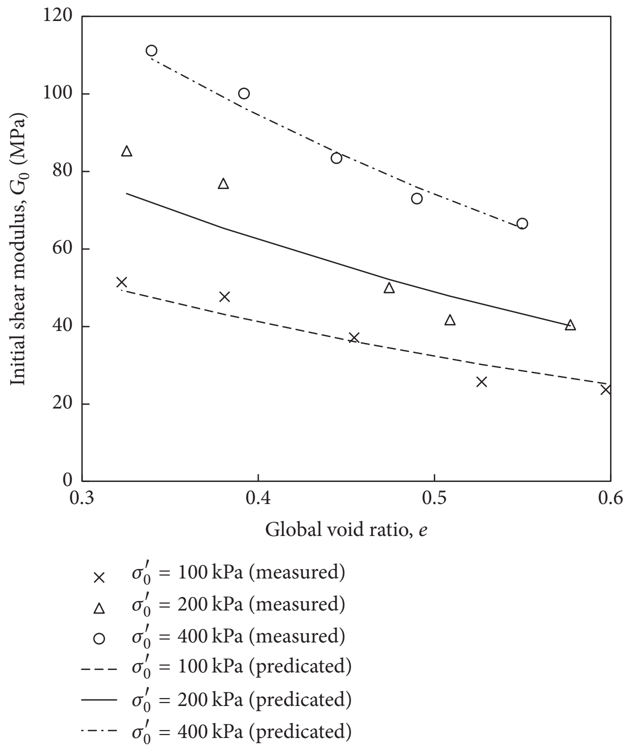

FIGURE 3: Comparison between computed and measured initial shear modulus.

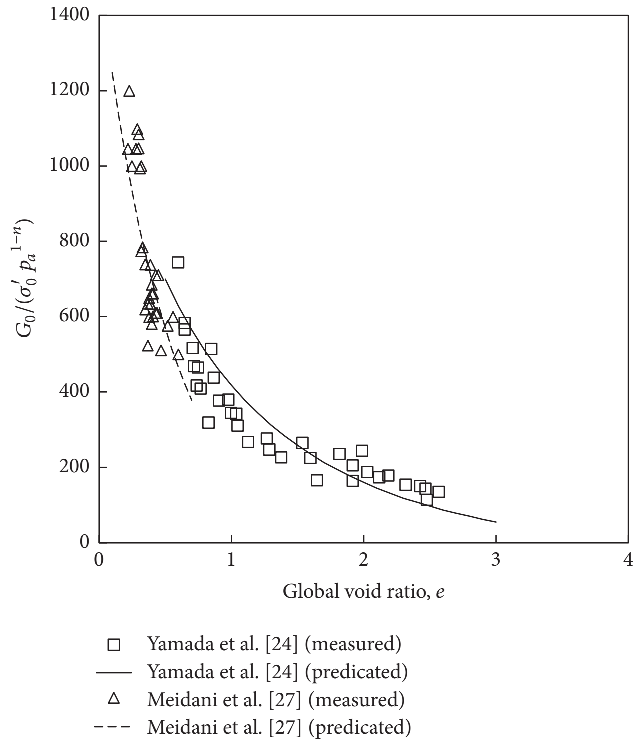

FIGURE 4: Comparison between computed initial shear modulus and literature data.

order to eliminate the influence of confining pressure, the initial shear modulus was normalized by $\sigma_0'^{n} \cdot p_a^{1-n}$ in the figure. Though the coarse particle sizes were different, there is a reasonably good correlation between the experimental and the calculated values. Equation (1) can be used to estimate the initial shear modulus of clay-aggregate mixtures; the effect of coarse aggregate content is reflected indirectly by the global void ratio.

3.2. Strain-Dependent Normalized Shear Modulus. The relationships between the normalized shear modulus G/G_0 and the shear strain amplitude γ at different confining stresses and coarse aggregate contents are shown in Figure 5. For each coarse aggregate content, the data points are observed to be basically distributed in a narrow belt zone; the influence of the confining stress on the normalized shear modulus of clay-aggregate mixtures is negligible. It is also observed that the coarse aggregate content has a significant effect on the normalized shear modulus. The rate of reduction in shear modulus with strain becomes faster as the coarse aggregate content increases. The similar observation has also been made by Yamada et al. [25]. One reason for this finding is that the clay-aggregate skeleton will collapse gradually due to the slippage between the clay and the coarse particles. Therefore, the effect of coarse particles in increasing the shear modulus will disappear gradually with the development of the shear strain; the shear modulus will be dominated by the clay fraction. Because the initial shear modulus increases with the increase in the coarse aggregate content, the samples with high coarse aggregate content have lower values of G/G_0 at a specific strain level.

From the above results, the following hyperbolic model was used to describe the relationship between the normalized shear modulus and the shear strain of clay-aggregate mixtures:

$$\frac{G}{G_0} = \frac{1}{1 + k_1 \left(1 + P/\left(a + bP\right)\right) \gamma}, \tag{2}$$

where k_1, a, and b are test parameters; P is the volume content of aggregates in decimal representation. The value of k_1 can be determined by the reciprocal of the shear strain at $G/G_0 = 0.5$ for the pure clay specimen. Parameters a and b are used to represent the effects of the coarse aggregate content. In this study, k_1, a, and b are obtained as 980, 0.24, and 0.37, respectively. The predicted $G/G_0 \sim \gamma$ relationships are also presented in Figure 5 as solid lines; the computed values are found to agree well with the test values.

3.3. Strain-Dependent Damping Ratio. The relationships between the damping ration D and the shear strain γ are shown in Figure 6. The results show that both the shear strain level and the coarse aggregate content have remarkable effects on the damping ratio, while the effect of the confining stress is negligible. It is observed that the damping ratio of the clay-aggregate mixture increased with increasing shear strain until a steady value $D_{\max}$ was reached. This observation is similar to the general trend of increasing equivalent damping ratio for pure clays.

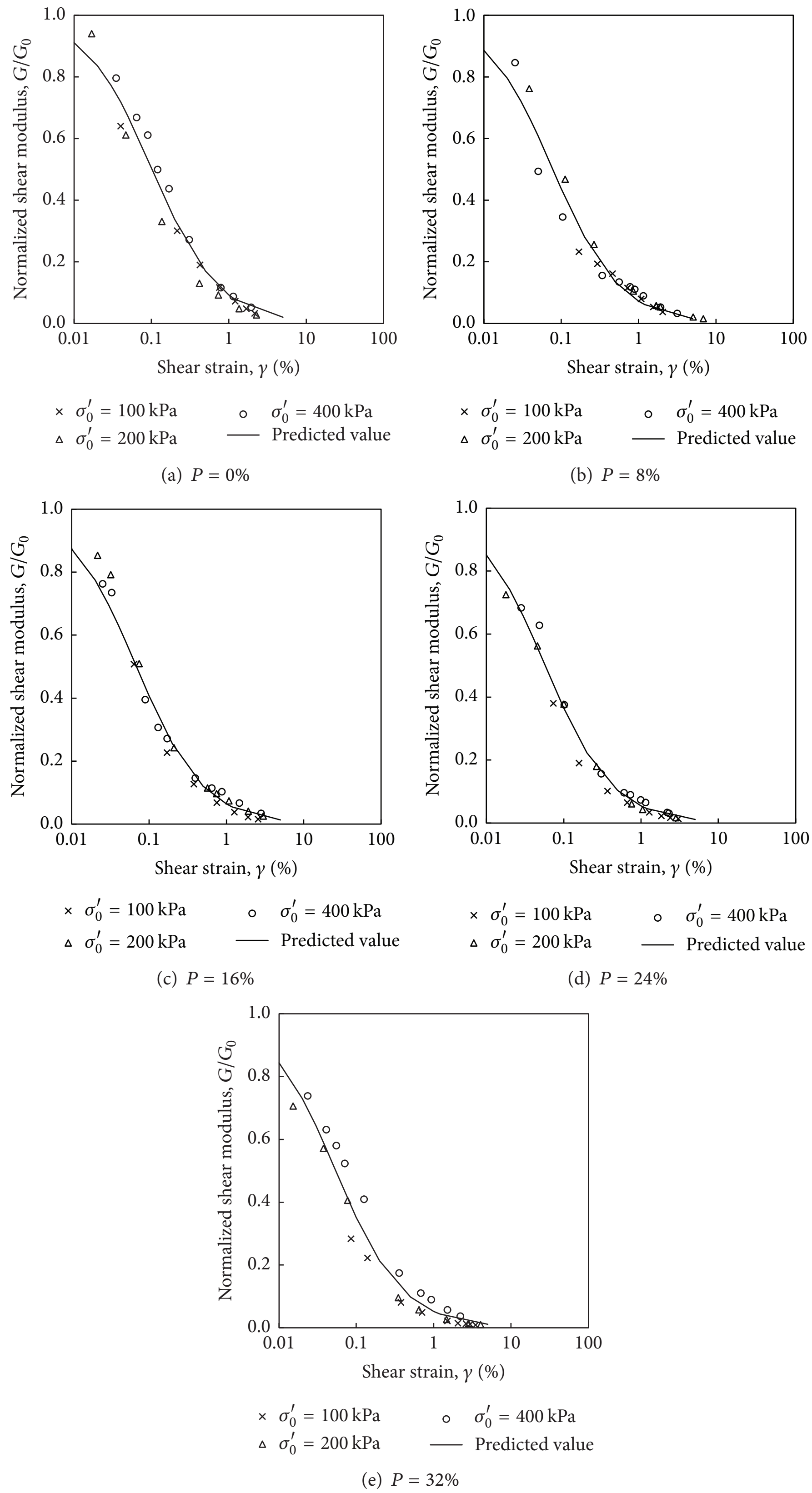

Figure 5: Relationship between normalized shear modulus and shear strain.

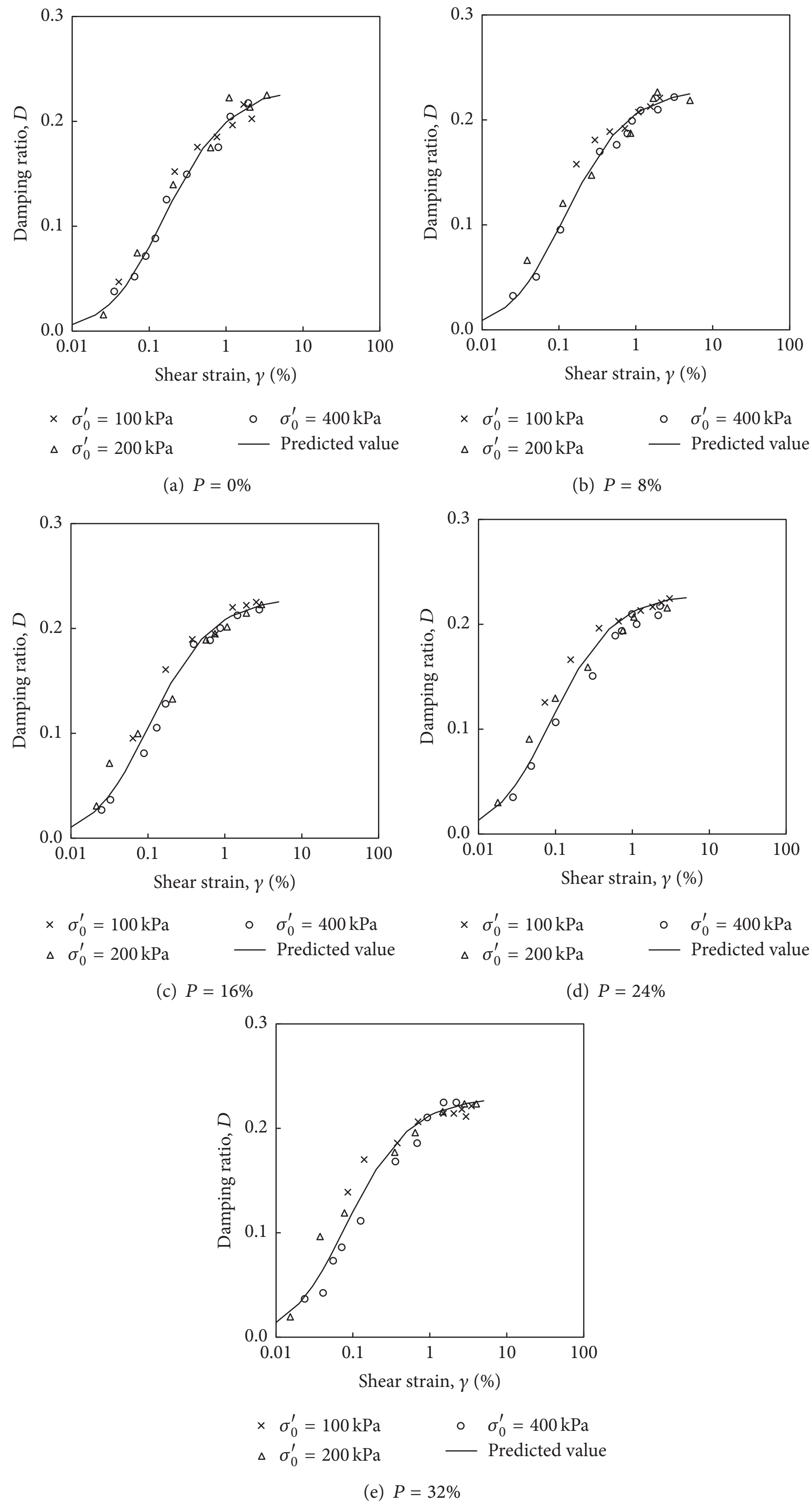

Figure 6: Relationship between normalized shear modulus and shear strain.

In addition to the material damping, the friction and the slippage at the clay-aggregate interface may contribute to the energy loss. Since the number of interfaces increased with the coarse aggregate content, samples with larger coarse aggregate content showed larger damping ratios. However, when the shear strain was large enough ($\gamma > 1\%$), the clay matrix has been fully sheared and the effect of coarse particles was negligible. The values of $D_{\max}$ of all samples are found to be approximately 0.23, which is close to the measured value of the pure clay. It should be noted that mixtures with extremely high coarse aggregate content may have a different trend, since the coarse particles will control the dynamic behavior in those cases.

Based on the test results, the following empirical relationship was proposed to estimate the damping ratio:

$$D = D_{\max}\left(1 - \frac{G}{G_0}\right)^{\beta}, \tag{3}$$

where G/G_0 is the normalized shear modulus computed by (2); $D_{\max}$ is the maximum damping ratio, which can be determined by the asymptotic value of the damping ratio curve; β is the test parameter. In this study, $D_{\max}$ and β were obtained as 0.23 and 1.5, respectively. The fitted curves are compared with the test data in Figure 6. The effect of the coarse particles on damping ratio curves is represented well by the normalized shear modulus at different coarse aggregate contents.

3.4. Cyclic Shear Strength. The cyclic axial strain (ε_d) time histories for the specimens with the coarse aggregate content of 0 and 32% (CSR = 0.15 and $\sigma_0' = 100$ kPa) are shown in Figure 7. As noted, the addition of coarse particles led to decreasing strain amplitude at a given loading cycle number. But the strain development characteristic did not change significantly. The induced strain amplitudes of both specimens were found to constantly increase with the loading cycles and a progressive failure type was observed. Therefore, it is concluded that the clay specimens mixed with the adopted coarse aggregate contents are unlikely to liquefy.

The relationships between the cyclic stress ratio (CSR) and the number of cycles corresponding to a double amplitude axial strain of 5% (N_f) are shown in Figure 8. It is found that the value of N_f increased significantly with the coarse aggregate content, especially at small values of CSR. For larger CSR values, the slippages at the clay-aggregate interfaces were more easy to develop. Hence, the effects of the coarse aggregate content on the resistance to deformation became less pronounced.

Usually, the cyclic shear strength is defined as the value of CSR corresponding to a specific failure number of loading cycles [31]. In this study, $N_f = 20$ is used to determine the cyclic shear strength, which corresponds to an earthquake magnitude of 7.5. Relationships between the cyclic shear strength CSR_{20} and the coarse aggregate content are plotted in Figure 9. It is clear that CSR_{20} increased rapidly with increasing coarse aggregate contents, though the dry density of the clay fraction was kept constant. The values of CSR_{20} were 0.15, 0.19, and 0.21 for the coarse aggregate content of 0%, 16%, and 32%, respectively.

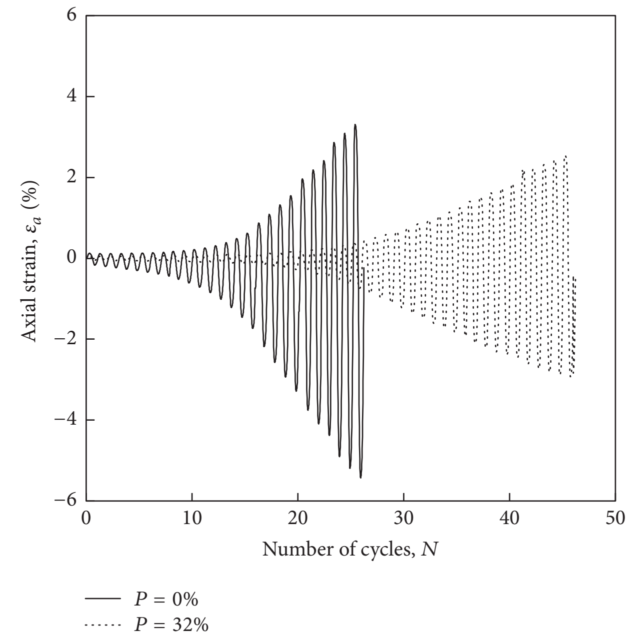

FIGURE 7: Time history of axial strain (CSR = 0.15; $\sigma_0' = 100$ kPa).

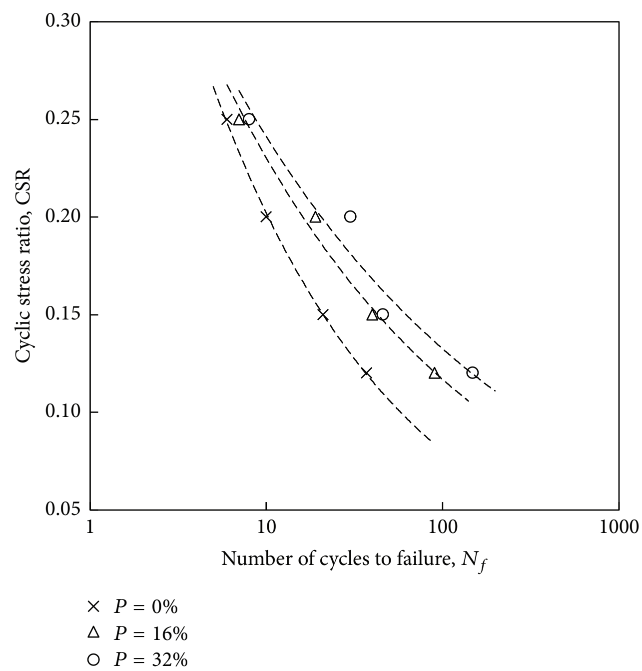

FIGURE 8: Relationship between cyclic stress ratio and number of cycles at failure.

3.5. Excess Pore Water Pressure. Figure 10 presents the time histories of the excess pore water pressure ratio r_u (defined as the ratio of the excess pore water pressure to the initial effective confining stress) of the specimens with the coarse aggregate content of 0 and 32% (CSR = 0.15 and σ_0' =

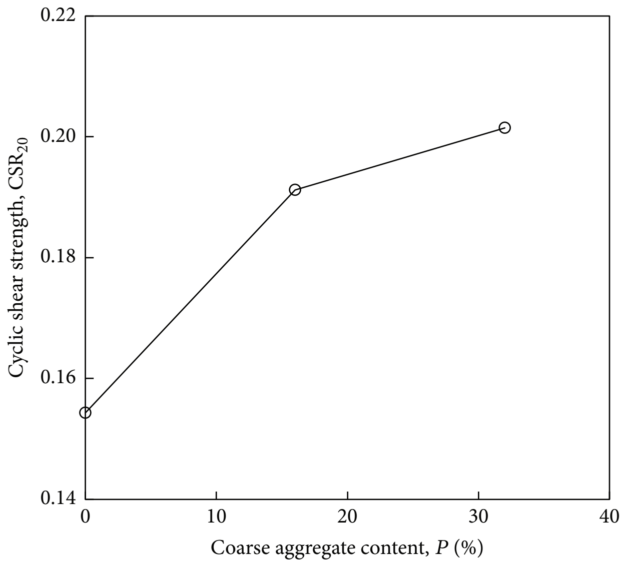

Figure 9: Relationship between cyclic shear strength and coarse aggregate content.

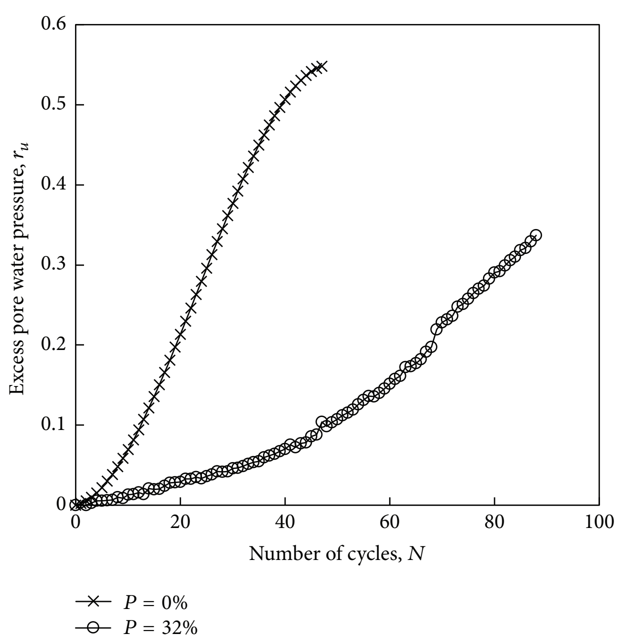

Figure 10: Time history of excess pore water pressure ratio (CSR = 0.15; $\sigma_0' = 100\,\text{kPa}$).

100 kPa). The excess pore pressures at the end of each cycle were given in the figure, such that the cyclic pore pressures due to variations of the mean stress are not included. As can be seen, the pore water pressures generated during the cyclic loading were not sufficient to trigger liquefaction for either the pure clay or the clay-aggregate mixture. For each coarse aggregate content, the rates of pore water pressure generation are approximately constant, which is consistent with the progressive-type failure behavior. Similar trends were also observed for the other specimens. It is also noted that the pore water pressure generated more slowly for the specimen

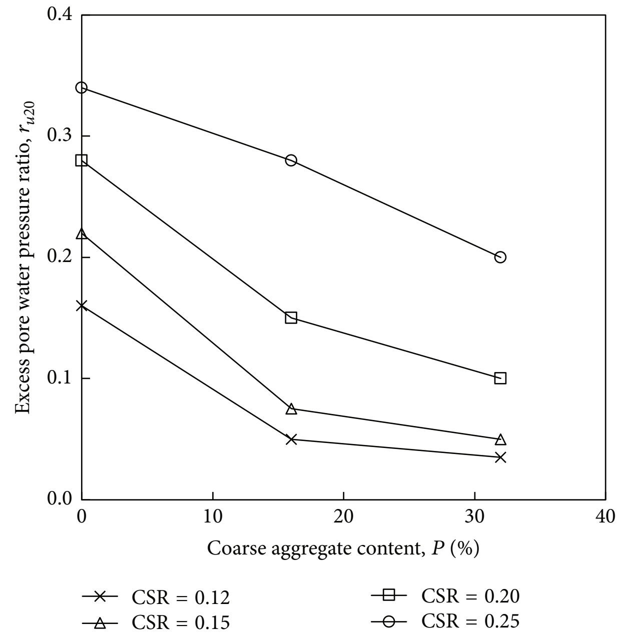

Figure 11: Relationship between excess pore water pressure ratio and coarse aggregate content.

mixed with coarse particles. It suggests that the soils with high coarse aggregate contents tend to be less contractive, causing a slower rate of excess pore water pressure generation.

The effects of the coarse aggregate content on the excess pore water pressure ratio are clearly shown in Figure 11, where the test results are presented in terms of r_{u20} (pore water pressure ratio for the 20th cycle) against the coarse aggregate content. It is obvious that the influence of the coarse aggregate content on r_{u20} also depends on the applied cyclic shear stress. At low cyclic shear stress (CSR $\leq$ 0.2), an increase of the coarse aggregate content led to a significant decrease in the generated excess pore water pressure. At large cyclic shear stress (CSR = 0.25), the soil skeleton consisting of clay and coarse particles was susceptible to collapse after a few loading cycles; then the pore water pressure generation was dominated by the clay fraction. Therefore, the same variation in the coarse aggregate content resulted in a small reduction in r_{u20}.

4. Conclusions

To improve the understanding of the dynamic behavior of clay-aggregate mixtures, series of stress controlled cyclic triaxial tests were performed on clay specimens mixed with different amounts of coarse particles. The main findings were as follows:

(1) The initial shear modulus increased with the coarse aggregate content, even though the dry density of the clay fraction was kept constant. The initial shear modulus of clay-aggregate mixtures can be estimated in terms of the global void ratio and the confining stress.

(2) The normalized shear modulus decreased and damping ratio increased with the increase in the coarse aggregate content. However, the effect of coarse particles was negligible at high shear stain levels. The empirical relationships to determine the strain-dependent normalized shear modulus and damping ratio were proposed.

(3) Adding coarse particles to a clay matrix led to increasing of the cyclic shear strength. At small cyclic stress ratios, the number of loading cycles to failure increased significantly with the coarse aggregate content. For large cyclic stress ratios, the effects of the coarse aggregate content on the resistance to deformation became less pronounced.

(4) The clays with high coarse aggregate contents tended to be less contractive, causing a slower rate of excess pore water pressure generation during the undrained cyclic loading. The decrease in the excess pore water pressure is especially significant at low cyclic shear stress levels.

Competing Interests

The authors declare that there is no conflict of interests regarding the publication of this paper.

Acknowledgments

The authors acknowledge support from the Natural Science Foundation of Jiangsu Province (no. BK20141279) and the Qing Lan Project by the Jiangsu Province Government.

References

[1] S. Thevanayagam, K. Ravishankar, and S. Mohan, "Effects of fines on monotonic undrained shear strength of sandy soils," *Geotechnical Testing Journal*, vol. 20, no. 4, pp. 394–406, 1997.

[2] L.-K. Chien, Y.-N. Oh, and C.-H. Chang, "Effects of fines content on liquefaction strength and dynamic settlement of reclaimed soil," *Canadian Geotechnical Journal*, vol. 39, no. 1, pp. 254–265, 2002.

[3] K. Kuwano, H. Nakazawa, K. Sugihara, and H. Yabe, "Undrained cyclic shear strength of sand containing fines," in *Proceedings of the 11th Japan National Conference on Geotechnical Engineering*, vol. 1, pp. 993–994, 1996.

[4] E. Ovando-Shelley and B. E. Pérez, "Undrained behaviour of clayey sands in load controlled triaxial tests," *Geotechnique*, vol. 47, no. 1, pp. 97–111, 1997.

[5] K. Ishihara, "Liquefaction and flow failure during earthquakes," *Geotechnique*, vol. 43, no. 3, pp. 351–415, 1993.

[6] M. A. A. Beroya, A. Aydin, and R. Katzenbach, "Insight into the effects of clay mineralogy on the cyclic behavior of silt-clay mixtures," *Engineering Geology*, vol. 106, no. 3-4, pp. 154–162, 2009.

[7] S.-S. Park and Y.-S. Kim, "Liquefaction resistance of sands containing plastic fines with different plasticity," *Journal of Geotechnical and Geoenvironmental Engineering*, vol. 139, no. 5, pp. 825–830, 2013.

[8] V. C. Xenaki and G. A. Athanasopoulos, "Liquefaction resistance of sand-silt mixtures: an experimental investigation of the effect of fines," *Soil Dynamics and Earthquake Engineering*, vol. 23, no. 3, pp. 1–12, 2003.

[9] I. B. Gratchev, K. Sassa, V. I. Osipov, and V. N. Sokolov, "The liquefaction of clayey soils under cyclic loading," *Engineering Geology*, vol. 86, no. 1, pp. 70–84, 2006.

[10] M. Derakhshandi, E. M. Rathje, K. Hazirbaba, and S. M. Mirhosseini, "The effect of plastic fines on the pore pressure generation characteristics of saturated sands," *Soil Dynamics and Earthquake Engineering*, vol. 28, no. 5, pp. 376–386, 2008.

[11] U. Kim, D. Kim, and L. Zhuang, "Influence of fines content on the undrained cyclic shear strength of sand-clay mixtures," *Soil Dynamics and Earthquake Engineering*, vol. 83, pp. 124–134, 2016.

[12] S. Thevanayagam, T. Shenthan, S. Mohan, and J. Liang, "Undrained fragility of clean sands, silty sands, and sandy silts," *Journal of Geotechnical and Geoenvironmental Engineering*, vol. 128, no. 10, pp. 849–859, 2002.

[13] J. F. Peters and E. S. Berney, "Percolation threshold of sand-clay binary mixtures," *Journal of Geotechnical and Geoenvironmental Engineering*, vol. 136, no. 2, pp. 310–318, 2010.

[14] A. F. Cabalar and W. S. Mustafa, "Behaviour of sand–clay mixtures for road pavement subgrade," *International Journal of Pavement Engineering*, pp. 1–13, 2015.

[15] A. F. Cabalar and W. S. Mustafa, "Fall cone tests on clay-sand mixtures," *Engineering Geology*, vol. 192, pp. 154–165, 2015.

[16] R. Salgado, P. Bandini, and A. Karim, "Shear strength and stiffness of silty sand," *Journal of Geotechnical and Geoenvironmental Engineering*, vol. 126, no. 5, pp. 451–462, 2000.

[17] A. F. Cabalar, "The effects of fines on the behaviour of a sand mixture," *Geotechnical and Geological Engineering*, vol. 29, no. 1, pp. 91–100, 2011.

[18] A. F. Cabalar and R. A. Hasan, "Compressional behaviour of various size/shape sand-clay mixtures with different pore fluids," *Engineering Geology*, vol. 164, pp. 36–49, 2013.

[19] J. Chu and W. K. Leong, "Effect of fines on instability behaviour of loose sand," *Geotechnique*, vol. 52, no. 10, pp. 751–755, 2002.

[20] S. Thevanayagam, "Intergrain contact density indices for granular mixes-I: framework," *Earthquake Engineering and Engineering Vibration*, vol. 6, no. 2, pp. 123–134, 2007.

[21] S. Yagiz, "Brief note on the influence of shape and percentage of gravel on the shear strength of sand and gravel mixtures," *Bulletin of Engineering Geology and the Environment*, vol. 60, no. 4, pp. 321–323, 2001.

[22] H. F. Zhao, L. M. Zhang, and D. S. Chang, "Behavior of coarse widely graded soils under low confining pressures," *Journal of Geotechnical and Geoenvironmental Engineering*, vol. 139, no. 1, pp. 35–48, 2013.

[23] K. Fei, "Experimental study of the mechanical behavior of clay-aggregate mixtures," *Engineering Geology*, vol. 210, pp. 1–9, 2016.

[24] S. Yamada, M. Hyodo, R. P. Orense, and S. V. Dinesh, "Initial shear modulus of remolded sand-clay mixtures," *Journal of Geotechnical and Geoenvironmental Engineering*, vol. 134, no. 7, pp. 960–971, 2008.

[25] S. Yamada, M. Hyodo, R. P. Orense, S. V. Dinesh, and T. Hyodo, "Strain-dependent dynamic properties of remolded sand-clay mixtures," *Journal of Geotechnical and Geoenvironmental Engineering*, vol. 134, no. 7, pp. 972–981, 2008.

[26] A. Shafiee and R. Ghate, "Shear modulus and damping ratio in aggregate-clay mixtures: an experimental study versus ANNs

prediction," *Journal of Applied Sciences*, vol. 8, no. 18, pp. 3068–3082, 2008.

[27] M. Meidani, A. Shafiee, G. Habibagahi et al., "Granule shape effect on the shear modulus and damping ratio of mixed gravel and clay," *Iranian Journal of Science and Technology, Transaction B: Engineering*, vol. 32, no. 5, pp. 501–518, 2008.

[28] M. M. Monkul and G. Ozden, "Compressional behavior of clayey sand and transition fines content," *Engineering Geology*, vol. 89, no. 3-4, pp. 195–205, 2007.

[29] R. K. McGeary, "Mechanical packing of spherical particles," *Journal of the American Ceramic Society*, vol. 44, no. 10, pp. 513–522, 1961.

[30] K. Ishihara, *Soil Behaviour in Earthquake Geotechnics*, Clarendon Press, Oxford University Press, 1996.

[31] B. Seed and K. L. Lee, "Liquefaction of saturated sands during cyclic loading," *Journal of Soil Mechanics & Foundations*, vol. 92, no. 6, pp. 105–134, 1966.